Vibration of Prestressed Membrane Reflectors

S. Kukathasan and S. Pellegrino

CUED/D-STRUCT/TR194

European Space Agency Contractor Report

The work presented in this report was carried out under an ESA contract.

Responsibility for its contents resides with the authors.

ESA Study Manager: W.J. Rits

ESTEC Contract no. 11936/96/NL/FG

Release date: 16 March 2001

Abstract

This report presents a study of the vibration behaviour of various prestressed membrane structures. A vibration analysis of flat membranes of arbitrary shape is done using the ABAQUS finite element package, and compared with analytical solutions; good agreement between the two solutions is obtained. The finite element model is then extended to the Collapsible Rib-Tensioned Surface Reflector, currently under development by the European Space Agency. Natural frequency and mode shape estimates are obtained for various reflector diameters, hub dimensions, number of ribs and prestress levels. The analysis results indicate that the fundamental natural frequency of the reflector decreases with the increase of diameter of the reflector and does not change greatly with the increase of hub radius. Furthermore, the fundamental natural frequency increases with the increase of membrane prestress. A periodic nature of variation in the results is observed.

Contents

List of Figures

List of Tables

Chapter 1

Introduction

The type of structures that is of interest in the present study is high-precision deployables for spacecraft, where there is a growing requirement for furlable reflecting surfaces for antennae, reflectors and solar arrays. The configurations that are being considered include both flat and curved surfaces. The performance efficiency of these reflective surfaces depends not only on the geometric accuracy of these surfaces but also on their vibration characteristics.

1.1 Scope of the report

The aim of this report is to develop methods for predicting the vibration behaviour of prestressed membrane structures of general shape, with a thickness of only a fraction of a millimetre. Numerical studies of the vibration of flat membranes provide a natural way of approaching this field. The predictive methods developed for flat membranes are then applied to predict the vibration behaviour of a deployable membrane reflector currently under development in the Deployable Structures Laboratory, at the University of Cambridge.

1.2 Layout of the Report

The layout of this report is as follows. Chapter 2 gives a brief overview of relevant previous work in the area of deployable membrane structures.

Chapter 3 presents a numerical and analytical study of simple flat membranes, plus a tubular structure consisting of four membrane elements. The modelling of prestressed membrane structures in ABAQUS is explained, including the selection of appropriate elements. The finite element results are compared to available analytical results for simple membranes and different ways of modelling the mem-

brane, e.g. as a grid of truss elements, are considered.

Chapter 4 presents a numerical study of CRTS reflectors. Estimates of the in-vacuum vibration of CRTS reflectors are obtained and, since no experimental results are currently available, the finite element analysis results obtained using continuum membrane elements are compared to a truss element model.

Chapter 5 concludes the report and identifies further work that should be carried out as a follow-on to this study.

Chapter 2

Literature Review

2.1 CRTS Reflector

A multipurpose deployable reflector, called the Collapsible Rib Tensioned Surface (CRTS) reflector, is being developed by the European Space Agency. A CRTS reflector, shown in Figure 2.1, consists of three main parts: a central expandable hub, a series of thin-walled foldable ribs connected radially to the hub and a membrane that is supported and tensioned by the ribs.

In the case of a symmetric reflector, the membrane consists of identical flat gores bonded together along their curved edges. When the reflector is deployed, each gore takes approximately the shape of a singly-curved cylindrical surface. The overall shape of a CRTS reflector is not an exact paraboloid but only an approximation to it, the accuracy of which improves as the number of gores is increased. Each rib consists of a thin slender metal blade with curved cross section. A key feature of this structural element is that it is continuous, and yet it can be folded elastically in several different ways.

The vibration characteristics of these reflectors, in the deployed configuration, are analysed in Chapter 4.

2.2 Periodic Structures

Periodic structures consist of a number of identical repetitive units linked in a similar pattern. Many complex engineering structures can be included in this category. The analysis of these structures can be simplified by considering their periodic nature. Because of the periodic nature of the CRTS reflector, previous work on the vibration analysis of periodic structures is briefly reviewed below.

Figure 2.2 shows the natural frequency estimation of an infinite periodic beam

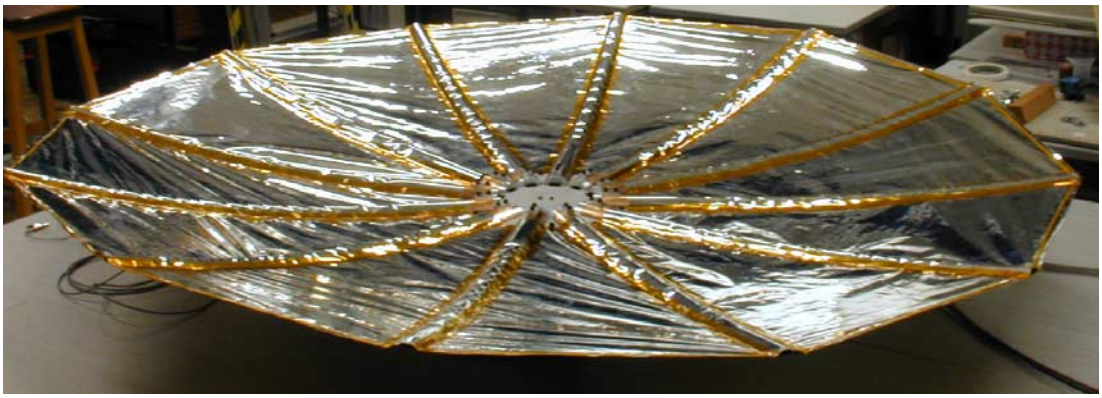

Figure 2.1: CRTS Reflector.

from its wave propagation relationship, which was studied by SenGupta [12, 13].

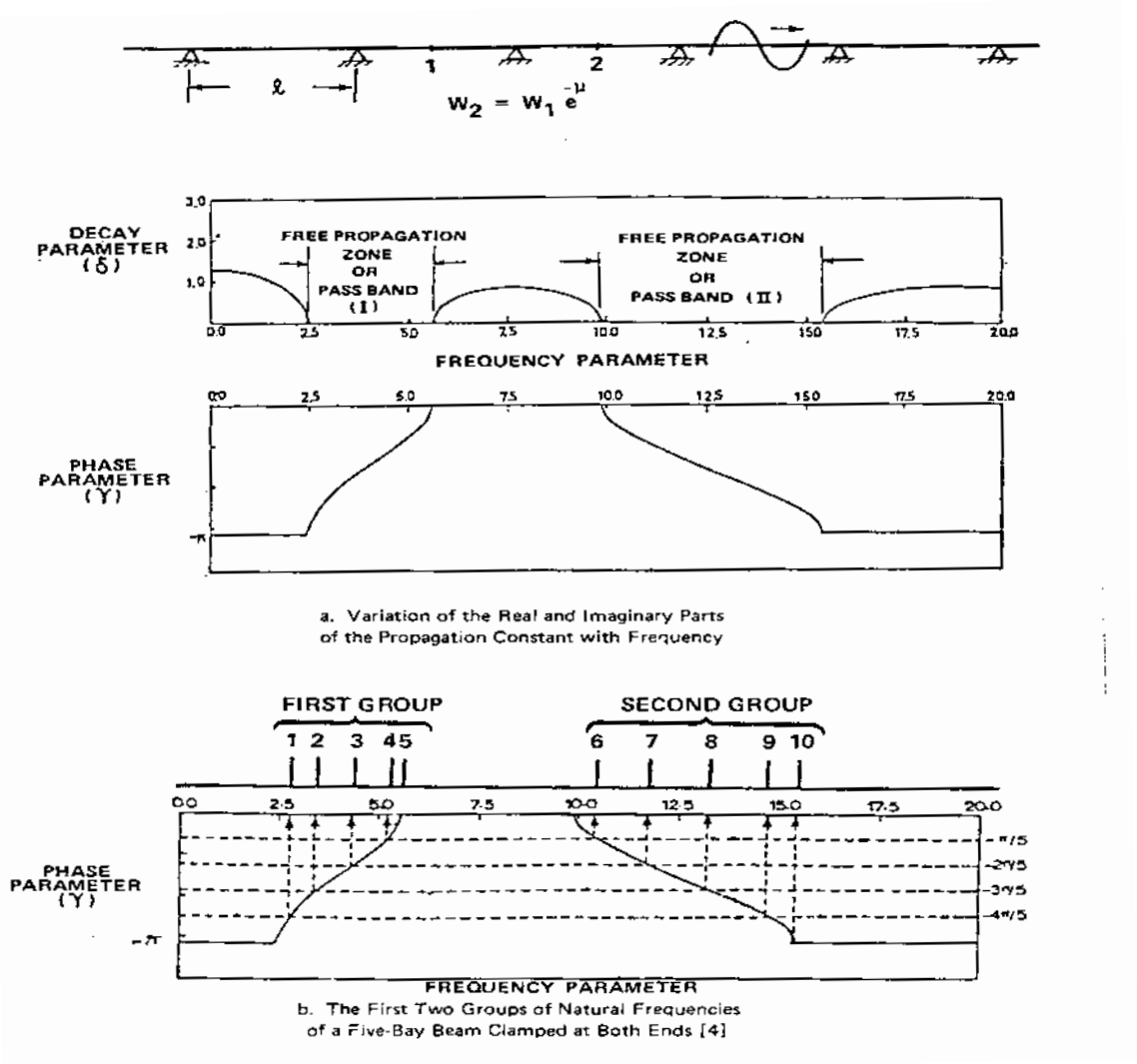

Figure 2.2: Natural frequencies of periodic beam (from SenGupta [13]).

For a flexural wave travelling from one bay to the next, the amplitudes at two points separated by a periodic distance can be related by

$$W_2 = W_1 e^{-\mu} \tag{2.1}$$

where μ is the propagation constant which is generally complex. The real part δ defines the rate of decay of the amplitudes from one support to the other and the imaginary part γ denotes the phase difference between the quantities at two successive supports.

Figure 2.2.a shows a typical plot of propagation constant vs. frequency parameter for a periodically supported infinite beam.

The natural frequencies of a five-span beam clamped at both ends are obtained [12] by applying boundary conditions on the bending moment at the end supports, thus obtaining γ as

$$\gamma = \frac{m\pi}{N} \tag{2.2}$$

where m is an integer which varies from 1 to N and N is total number of spans, i.e. in this case N=5.

Figure 2.2.b gives the first two groups of natural frequencies of the five-span beam. The results are obtained from Equation (2.2) and Figure 2.2.a. An important feature of these results is that the number of normal modes (or natural frequencies) in a given propagation zone (or in a group) is equal to the number of spans. The natural frequencies of a beam with N-spans can similarly be obtained from the same plot of γ vs. frequency parameter, by dividing the ordinate into N equal parts and reading the corresponding projections on the abscissa.

As explained above, periodic structures have the advantage of simplifying the dynamic analysis. But in reality, almost all practical structures have small irregularities because of manufacturing and material tolerances. These structural irregularities can significantly affect the vibration behaviour of nearly periodic structures, by localising the vibration modes and confining the energy to a region close to the source. This phenomenon is generally called *mode localisation*.

The mode localisation of a 15 m diameter space reflector with various number of ribs has been investigated numerically by Cornwell and Bendiksen [4]. In their study, the 18-rib reflector did not localise in the first mode but the higher modes did, and the localisation became progressively more severe with increasing mode number. When the number of ribs was increased to 48, the localisation became even more severe. This indicates the importance of considering mode localisation on a large space reflector having many ribs. More recent references in the area of mode localisation and energy confinement can be found in Yap and Cebon [14].

Chapter 3

Analysis of Membrane Structures

This chapter describes a numerical study of the vibration of flat membranes and a simple membrane tubular structure. Natural frequencies of flat membranes are obtained from three different methods, one analytical and two computational, in Section 3.1. In Section 3.2 the two different approaches are applied to the calculation of the natural frequencies of a simple tubular structure consisting of four flat membranes.

3.1 Flat Membranes

Three flat membrane shapes (square, triangle and L-shape) are studied, focusing in particular on the variation of the fundamental natural frequency with the level of pre-tension.

The fundamental natural frequencies are calculated using three different methods: an analytical method, the Finite Element (FE) method using membrane elements and the FE method using truss elements. The results obtained with membrane elements are compared to analytical results and FE results with truss elements.

3.1.1 Analytical Method

The natural frequencies of the rectangular, triangular and L-shaped membranes shown in Figure 3.1 are obtained as follows.

Consider the transverse vibration of a thin and uniform rectangular flat membrane that is in equilibrium, in a planar configuration, under a uniform tension T per unit length. The transverse displacement of any point on the membrane is in the direction normal to the reference surface and is assumed to be small; as a result the tension in the membrane can be assumed to be constant. Defining a

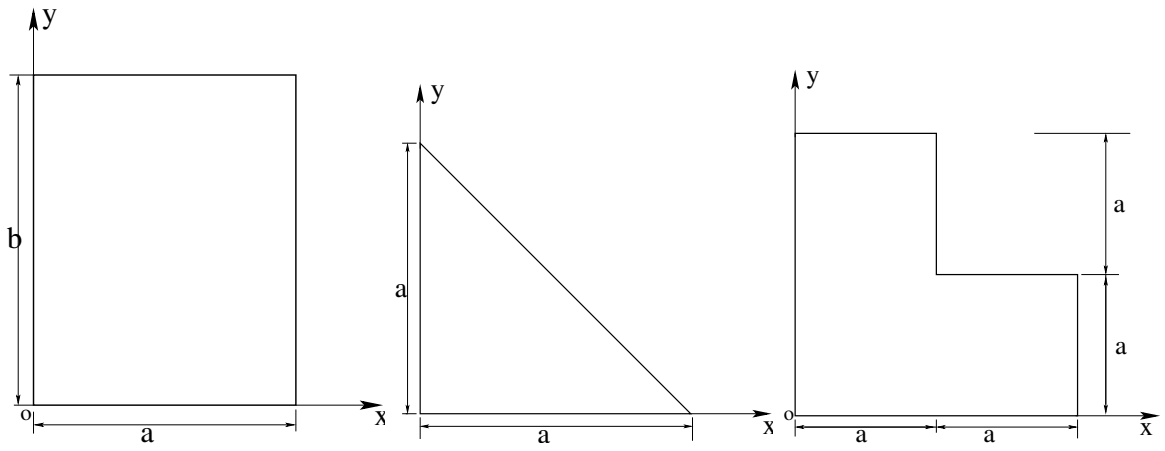

(a) Rectangle (b) Triangle (c) L-shape

Figure 3.1: Flat membranes.

coordinate system O, x, y with origin O at a corner and axes parallel to the sides of the rectangle shown in Figure 3.1(a), the governing equation of transverse motion can be written as [6, 11];

$$T(\frac{\partial^2 \eta}{\partial x^2} + \frac{\partial^2 \eta}{\partial y^2}) = M \frac{\partial^2 \eta}{\partial t^2} \tag{3.1}$$

where η is the transverse displacement of the membrane at point (x, y), T is the uniform surface tension per unit length and M is the mass per unit area of the membrane.

For steady-state vibration at a frequency ω, the transverse displacement at a point (x, y) at time t can be specified as,

$$\eta_{(x,y,t)} = \eta_{(x,y)} \cos \omega t \tag{3.2}$$

For a simply supported rectangular membrane η=0 along the boundaries, hence the mode shape is sinusoidal in both directions. Therefore, the transverse displacement η at a point (x, y) has the expression

$$\eta_{(x,y,t)} = \sin \frac{m\pi x}{a} \sin \frac{n\pi y}{b} \cos \omega t \tag{3.3}$$

Substituting Equation (3.3) into Equation (3.1) and solving for the natural frequency of vibration ω, we obtain

$$\omega_{mn} = \pi c \sqrt{\frac{m^2}{a^2} + \frac{n^2}{b^2}} \tag{3.4}$$

where m, n are integers, c the wave propagation velocity in the membrane, and c is defined as

$$c = \sqrt{\frac{T}{M}} \tag{3.5}$$

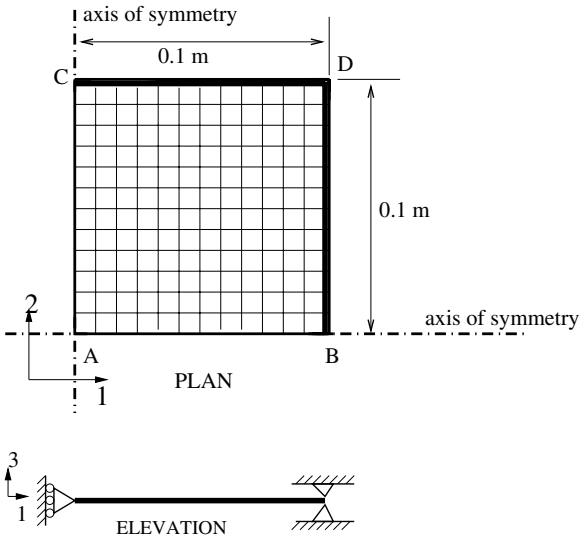

Figure 3.2: Quarter portion of square membrane.

Similarly, the analytical expression for the natural frequency of the right-angled triangular membrane shown in Figure 3.1(b) is [1]

$$\omega_{mn} = \pi c \sqrt{\frac{m^2 + n^2}{2A}} \tag{3.6}$$

where A is the area of the triangle.

The L-shaped membrane shown in Figure 3.1(c) has the following fundamental natural frequency [1]

$$\omega_1 \approx \pi c \frac{1.717}{\sqrt{A}} \tag{3.7}$$

where A is the area of the L-shaped membrane.

3.1.2 FE Analysis with Membrane Elements

The formulation of an analytical model for a membrane structure, although straightforward for the rectangular flat membrane described in the previous section, can be extremely difficult for structures having complex geometry. The finite element (FE) method overcomes these difficulties. A detailed explanation of the FE method in structural dynamics can be obtained from references [2,3,5].

Flat membranes of three different shapes (square, triangular and L-shaped) were analysed using the FE package ABAQUS [7]. The square membrane has a side length of 0.2 m and a thickness of 0.1 mm; it is supported on knife edges, which act as simple supports along all four edges. Only one quarter of the membrane is considered, as shown in Figure 3.2, since the membrane is symmetrical.

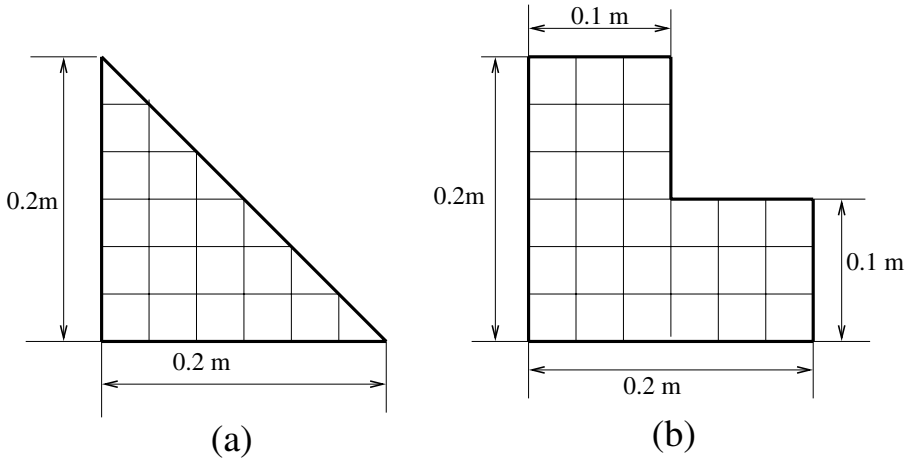

Figure 3.3: Triangular and L-shaped membranes.

The triangular membrane has base length of 0.2 m and height of 0.2 m; it is supported on knife edges along all three edges, see Figure 3.3(a). The L-shaped membrane (base length of 0.2 m) is also supported on knife edges along all six edges, see Figure 3.3(b).

These three membranes are modelled using two different elements available in ABAQUS: the M3D4 membrane element, a 4 node quadrilateral element, and the M3D3 membrane element, a 3 node triangular element. Both are plane stress elements that transmit in-plane forces only (no moments) and have no bending stiffness. This means that it is necessary to prestress these elements before any vibration analysis is carried out. The material is assumed to be Kevlar-reinforced Kapton foil whose properties are tabulated in Table 3.1.

The mesh for the square membrane, shown schematically in Figure 3.2, consists of square elements. Note that the number of elements will be kept at 100, as only a small variation in frequency was observed when the number of elements was increased to 1600, which —of course— required much longer computation times.

The following boundary conditions are applied: the nodes along edges CD and BD are restrained in the 3-direction (vertical direction) to simulate simple supports, the nodes along edge AB are restrained in the 2-direction because of symmetry, and similarly the nodes along edge AC are restrained in the 1-direction. All other nodes are unrestrained.

Uniform biaxial prestress is applied to the membrane elements directly, using the **INITIAL CONDITIONS, TYPE=STRESS* option. This option is used before applying any of the **STEP* options. To account for the geometric stiffness induced by the prestress, non-linear calculation procedures are used. Hence, before the eigenvalue extraction calculations a non-linear static analysis step is carried out by using the **STEP, NLGEOM* option after the **INITIAL CONDITIONS* option. In the above static analysis step, the applied initial prestress is maintained by

initially restraining the outer edges of the membrane. Then, in the next step (frequency extraction step), the boundary conditions are changed to the actual ones, described above, by using **BOUNDARY, OP=NEW* option.

The frequency analysis step is a linear step, therefore the non-linear option is not used here. In this option, the user can request the number of eigenvalues to be extracted, and the choice of eigensolver. Of the two solution methods available in ABAQUS, the subspace iteration method and the Lanczos method, the Lanczos eigensolver is faster and more effective for models with many degrees of freedom [7,9] and therefore it was chosen. A sample ABAQUS script is included in Appendix A.

3.1.3 FE Analysis using Truss Elements

This analysis was performed to test the accuracy of the membrane element results, because in the case of complex membrane structures there is no reliable analytical estimate. The idea is to establish the accuracy of the truss model for flat membranes, so that it can be used to produce independent estimates, later on.

The equivalent truss model for static problems was initially implemented by Hrennikoff [8] and later used by Phaal [10] to analyse shell structures. The basic idea of the method consists in: (i) replacing a continuous elastic body by a truss of pin-jointed bars, arranged according to a definite pattern, whose elements are endowed with elastic properties suitable to the type of problem; (ii) analysing the framework; and (iii) spreading the bar stresses over the corresponding areas of the continuous body, in order to obtain the stresses in the original body. The framework so formed is given the same external outline and boundary restraints, and is subjected to the same loads as the solid body. Hrennikoff [8], has developed this analogy for elasto-statics, but the equivalence of density was not discussed in his paper. In the present study the density of the truss model is important for the frequency analysis. This problem is solved by considering the volume of material in a membrane panel and in the corresponding equivalent truss model. It is important, of course, to check that the two models have equal mass.

The equivalent truss model set up by Hrennikoff is based on the doubly-braced square framework shown in Figure 3.4(b), it has the same properties in both directions of the axes and has two characteristic cross-sectional areas A and A_1. Consider a membrane of Young's Modulus E, Poisson's ratio ν, thickness t and density ρ.

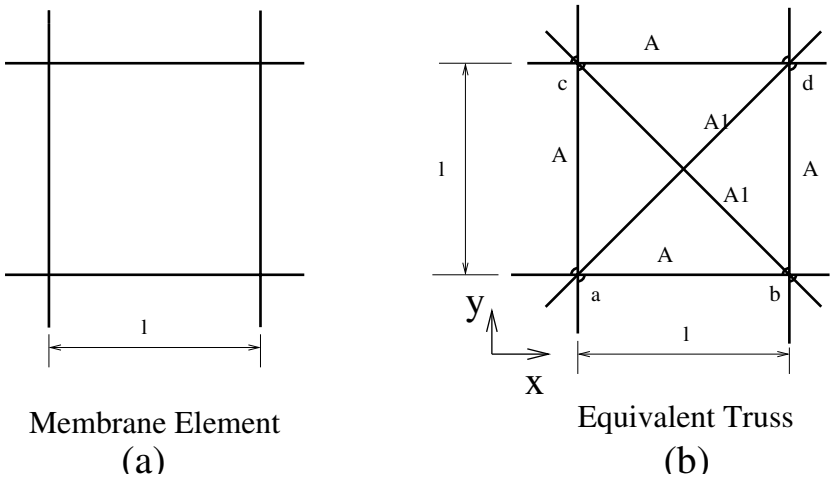

Figure 3.4: Equivalent truss model.

The values of A and A_1 can be derived from [8];

$$A = \frac{3}{4}lt \tag{3.8}$$

$$A_1 = \frac{3}{4\sqrt{2}}lt \tag{3.9}$$

where t is the thickness of the membrane. In the derivation E and ν are assumed to be same for both membrane element and equivalent truss.

The density of the bars of the truss (ρ_t) is estimated by equating the masses of the membrane and its equivalent truss model, hence

$$\rho_t = \frac{1}{3}\rho \tag{3.10}$$

Table 3.1: Properties of membrane and equivalent truss model.

Parameter	Membrane	Truss
Density (kg/m^3)	790	263
Young's Modulus (GPa)	11.9	11.9
Poisson's Ratio	0.3	0.3
Thickness (mm)	0.1	—

The equivalent truss shown in Figure 3.5 has been modelled using the 3-D truss elements (T3D2) available in ABAQUS. The biaxial prestress of 10 N/m is applied in the horizontal and vertical directions, i.e. 0.05 N in each horizontal bars, 0.035 N in each diagonal bars and 0.05 N in each vertical bars, using initial conditions

and procedures similar to those explained in the description of the membrane element.

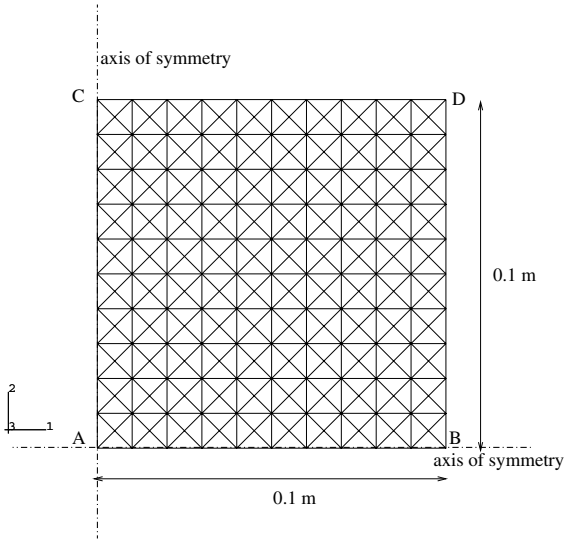

Figure 3.5: Equivalent truss model for square membrane.

3.1.4 Results

The fundamental natural frequency of the square membrane has been calculated for prestress levels of 10, 20, 30, 40 and 50 N/m, for 100 element and 1600 element models. The truss model shown in Figure 3.5 has also been analysed. The results are tabulated in Table 3.2.

Table 3.2: Estimates of fundamental natural frequency of square membrane.

Prestress (N/m)	FE Membrane (Hz)		FE Truss (Hz)	Analytical (Hz)
	100 Elements	1600 Elements		
10	39.66	39.76	39.73	39.78
20	56.08	56.23	56.19	56.25
30	68.69	68.87	68.81	68.90
40	79.31	79.52	79.46	79.56
50	88.67	88.90	88.84	88.95

The fundamental natural frequencies of the triangular and L-shaped membranes with prestress of 10 N/m have been calculated also with ABAQUS and with Equations (3.6) and (3.7). Their values are tabulated in Table 3.3.

Table 3.3: Estimates of fundamental natural frequency of various membranes.

Model	FE (Hz)	Analytical (Hz)
Square	39.66	39.78
Triangle	61.60	62.90
L-shape	55.44	55.77

3.2 Simple Membrane Structure

The structure shown in Figure 3.6 consists of two main parts: four 1 m long vertical ribs fixed at the bottom, and a thin membrane square tube that is supported and tensioned by the ribs. The ribs have circular cross-section of 2 mm radius; the membrane has a thickness of 0.1 mm and each panel is 0.5 m wide. The membrane is prestressed by applying a biaxial tension of 100 N/m in the horizontal and vertical directions before the frequency analysis is carried out.

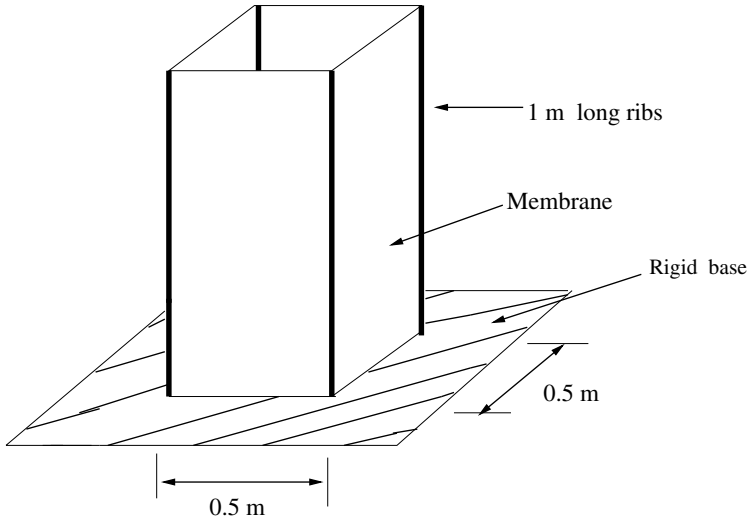

Figure 3.6: Simple membrane structure.

The natural frequencies of this structure, obtained from two different approaches, are compared to check the accuracy of the membrane element calculations in ABAQUS.

3.2.1 FE Analysis

The ribs are modelled with $B33$ beam elements. These are Euler-Bernoulli beam elements based on cubic interpolation functions, which do not allow for transverse shear deformation. They are reasonably accurate for cases involving distributed loading along the beam. The material of the ribs is steel, see Table 3.4. The membrane is modelled using the four node membrane elements (M3D4) described in Section 3.1.2. The material properties of the membrane are specified in Table 3.4.

A biaxial prestress of 100 N/m is applied to all four faces of the structure, as already mentioned in Section 3.1.2. When the prestress is applied, all four edges of the membranes are held fixed. Therefore, the prestress is "locked" into the membrane before the frequency analysis is carried out. In the frequency analysis step, the previously fixed edges are released and the actual boundary conditions are applied.

Table 3.4: Properties of ribs and membrane.

Parameter	Rib	Membrane
Density (kg/m^3)	7000	1
Young's Modulus (GPa)	200	20
Poisson's Ratio	0.3	0.3

The analysis has been repeated using the truss element model shown in Figure 3.7. The model consists of 3-D truss elements (T3D2) with an initial biaxial prestress of 100 N/m in the horizontal and vertical directions, i.e. 5 N in each horizontal bar, 3.54 N in each diagonal bar and 5 N in each vertical bar.

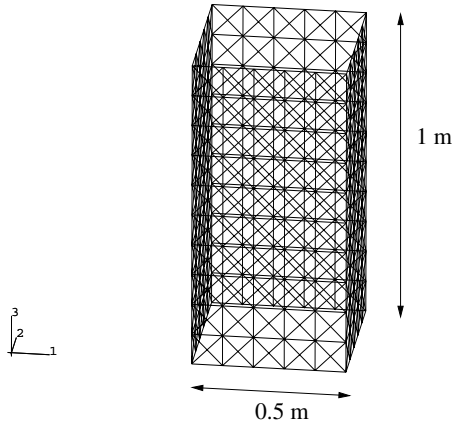

Figure 3.7: Equivalent truss model.

3.2.2 Results

Table 3.5 lists the natural frequencies obtained from the two methods, for biaxial prestress of 100 N/m.

The first four mode shapes of the membrane structure are plotted in Figures 3.8 and 3.9.

Table 3.5: Natural frequencies of simple structure.

Modes	Natural Frequency (Hz)	
	Membrane Model	Truss Model
1	289.54	288.04
2	309.80	309.51
3	309.83	309.51
4	333.11	334.42
5	804.18	785.12
6	828.95	826.84
7	828.95	826.84
8	828.95	829.59
9	828.95	829.59

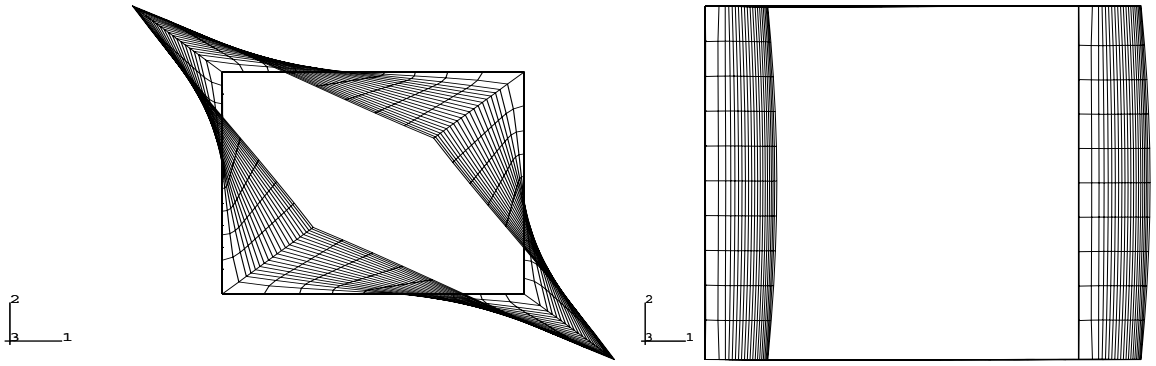

(a) Mode 1 (289.54 Hz)

(b) Mode 2 (309.80 Hz)

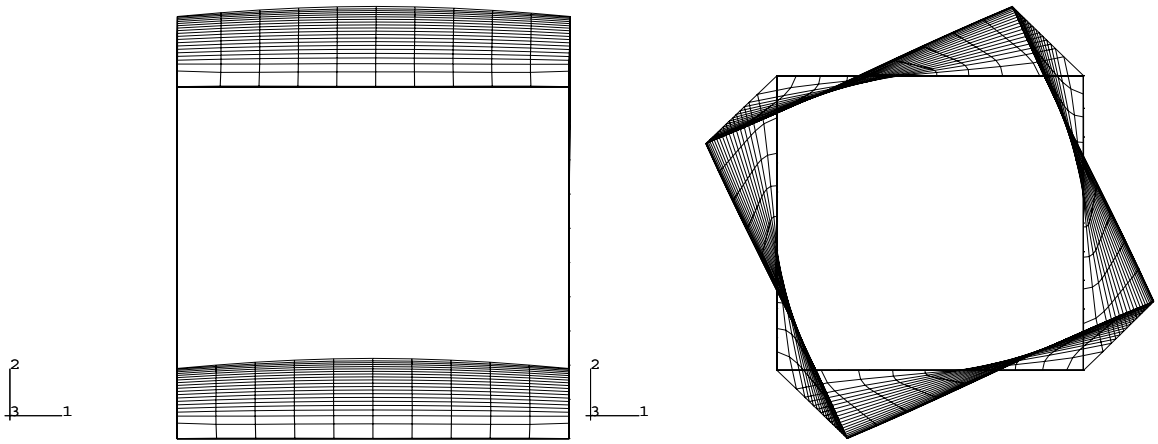

(c) Mode 3 (309.83 Hz)

(d) Mode 4 (333.11 Hz)

Figure 3.8: Top views of first four mode shapes.

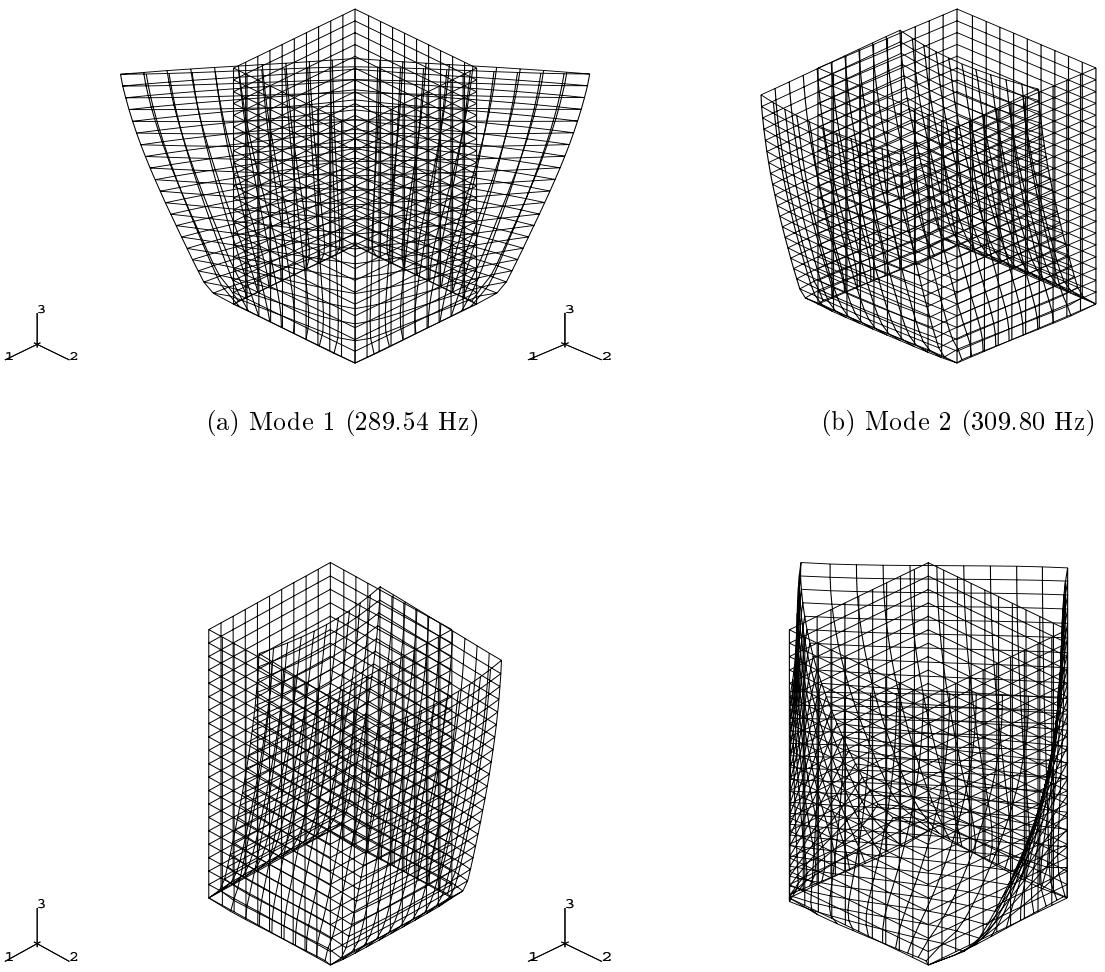

(a) Mode 1 (289.54 Hz)

(b) Mode 2 (309.80 Hz)

(c) Mode 3 (309.83 Hz)

(d) Mode 4 (333.11 Hz)

Figure 3.9: Isometric views of first four mode shapes.

3.3 Discussion

For the flat membrane results note —Table 3.2— that the FE results for different mesh densities show only a very small difference in frequency, although the finer mesh requires a much large computational time. Therefore, these results justify the use of moderately coarse meshes in further work.

The three sets of results in Table 3.2 show good agreement between FE and analytical solutions. This suggests that ABAQUS can be used reliably to estimate natural frequencies using the four node membrane elements M3D4. It can also be concluded that the truss model based on element T3D2 is broadly in agreement with the other models. Finally, Table 3.2 shows that the fundamental natural

frequency of the membrane increases with the applied prestress; this is because its geometric stiffness increases with prestress. Similar observations can be made from Table 3.3, for the triangular and L-shaped membranes.

For the simple membrane structure of Section 3.2 it can be observed in Table 3.5 that the membrane model and the truss model give similar results, with the exception of the fifth mode.

From these studies, it is clear that the ABAQUS membrane element M3D4 can be used to analyse membranes and membrane structures of any shape.

Chapter 4

Analysis of CRTS Reflectors

This chapter presents a study of the natural frequencies of a deployable membrane reflector antenna, in the deployed configuration. The effects of changing the diameter, hub radius and membrane prestress on the fundamental natural frequency are studied using ABAQUS. Results are presented for 1.5, 5 and 10 m diameter reflectors with 6, 12 and 24 ribs. Section 4.1 briefly introduces the reflector. The modelling and analysis of the reflector with ABAQUS are explained in Section 4.2. Section 4.3 presents the results that have been obtained, including a comparison between membrane and truss element models. A discussion of these results follows in Section 4.4.

4.1 Introduction

CRTS reflectors are generally lightweight and flexible, and there is the possibility that vibration of the reflector in the deployed configuration, induced by the attitude control system of the spacecraft, may degrade its intended performance. The dynamic response of a structure is mainly dependent on the coupling between dynamic loads exerted on the structure and the dynamic characteristics of the structure itself. If the frequency of the exciter is close to one of the natural frequencies of a structure, the maximum response of the structure will be induced. Therefore in the design of large deployable appendages it is customary to change the mass and stiffness distribution of the appendage to move the natural frequencies away from the rigid-body frequencies of the spacecraft. This approach is widely used in the dynamic design of reflector structures and, therefore, knowledge of the natural frequencies of CRTS reflectors plays an essential role in their design.

A special feature of symmetric CRTS reflectors (not those with offset configuration) is their periodic nature. A symmetric reflector consists of a number of identical repetitive units, or substructures. Therefore its analysis can be simpli-

Table 4.1: Material properties of ribs and membrane.

Parameter	Ribs	Membrane
Density (kg/m^3)	8400	790
Young's Modulus (GPa)	131	11.9
Poisson's Ratio	0.3	0.3
Thickness (mm)	0.2	0.1

fied considerably by considering its periodic nature [12, 13]. But in the actual model perfect periodicity cannot be achieved and even small imperfections in the model can cause the predictions of the natural frequency and mode shapes to be completely incorrect [4]. Although this is beyond the scope of the present study, it is clear that an experimental analysis will have to be carried out later on.

Returning to the vibration problem, it is impossible to obtain analytical (exact) solutions of the reflector, hence finite element (approximate) solutions will be used. The accuracy of these solutions will be assessed by modelling the reflector using both membrane elements (M3D4) and truss elements (T3D2) in the ABAQUS simulations, and by comparing the results.

4.2 Finite Element Modelling

The shape of the reflector is assumed to be a paraboloid, whose equation is given by

$$Z = \frac{X^2 + Y^2}{4F} \tag{4.1}$$

where Z is the height above the $X - Y$ plane, and the X, Y the Cartesian co-ordinates are measured from the centre of the reflector. F is the focal length, D the diameter. Reflectors with

$$\frac{F}{D} = 0.78 \tag{4.2}$$

are considered. The membrane of the reflector is Kevlar-reinforced Kapton foil and the ribs are made of Copper-beryllium. Their material properties are given in Table 4.1.

Several different configurations of the reflector are considered: 6, 12, 24 ribs, and 1.5, 5 and 10 m diameters. The membrane is assumed to be singly-curved between neighbouring ribs.

The nodal coordinates of a gore are defined using a MATLAB program. These nodes define a set of triangular elements. The nodal co-ordinates of the remaining gores are created using the **NCOPY, SHIFT, MULTIPLE="no. of gores"* option available in ABAQUS. After defining the element numbers for the first gore, the

element numbers of the remaining gores are simply created using the ABAQUS option **ELCOPY, OLD SET=() , SHIFT NODE=() , ELEMENT SHIFT=() , NEW SET=()*.

It is necessary to define a local axis parallel to the base of each gore in order to be able to define a prestress in the "hoop" direction. The initial prestress is applied in each gore in the local axis direction-1, parallel to the base, using the option **INITIAL CONDITIONS, TYPE=STRESS*. Along the ribs two sets of coinciding nodes are defined, one in each gore; these nodes are tied together using the option **MPC* .

The triangular membrane elements are modelled using M3D3 membrane elements. The ribs are modelled with B33 beam elements. The ribs have open-section with 0.2 mm thickness; their cross-section is shown in Figure 4.1. The rib cross-section is specified using the option **BEAM SECTION, SECTION=ARBITRARY* and the 5 points of the cross-section are specified in the next line of the input file. Figure 4.1 shows the actual cross-section of the rib, and the approximated cross-section. The orientation of the beam cross-section is defined in terms of a local, right handed axis system. This is achieved by defining the approximate rib direction in the option **BEAM SECTION*.

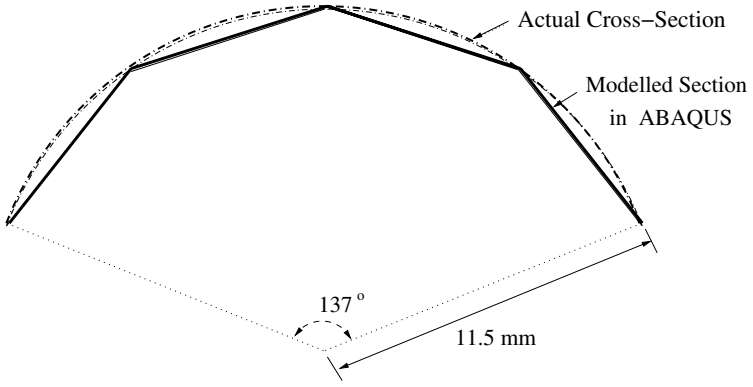

Figure 4.1: Actual and modelled shape of rib cross-section.

The finite element model of a 1.5 m diameter reflector with 12 ribs is shown in Figure 4.2.

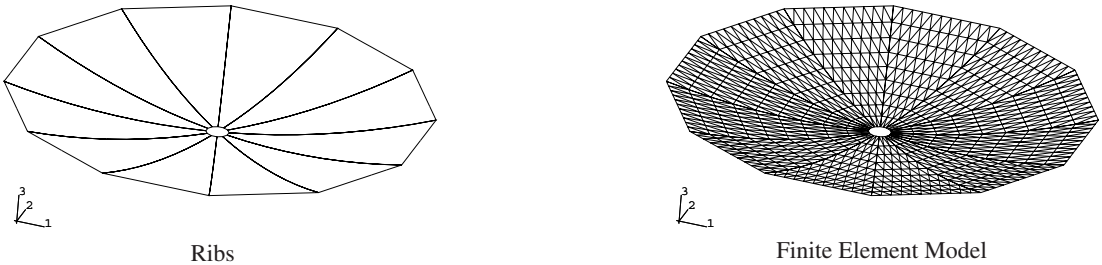

Figure 4.2: Model of 1.5 m diameter reflector with 12 ribs.

For the 1.5 m diameter reflector the frequency analysis has been done also for prestress levels of 50 N/m and 200 N/m, using the minimum value of the hub radius for each given number of ribs. This value is calculated by considering the minimum hub size required to accommodate the required number of ribs, but without allowing for the hub expansion during prestressing. Figure 4.3 shows a top view of the hub region defining the minimum hub radius for the case of 6 ribs.

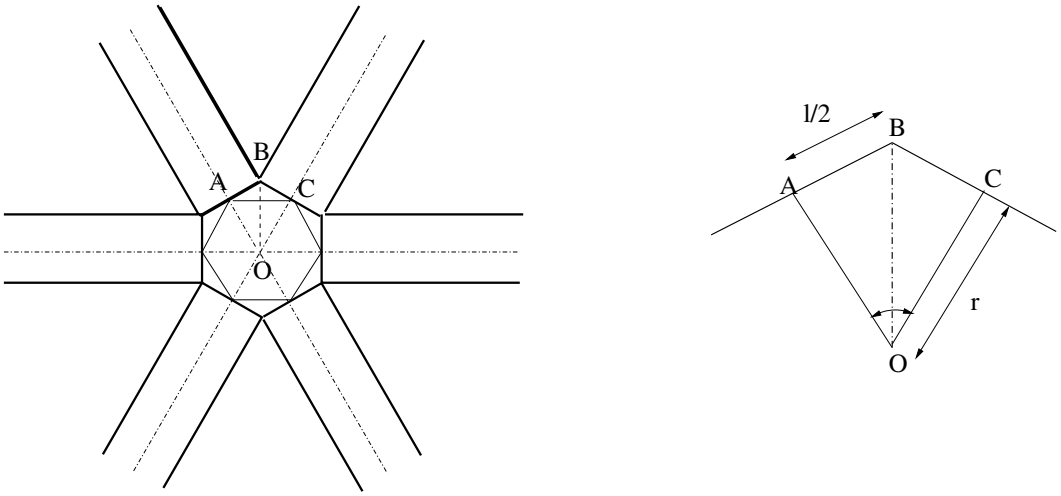

Figure 4.3: Minimum hub radius configuration.

Consider triangle OAB,

$$\tan\frac{\theta}{2} = \frac{l}{2r} \tag{4.3}$$

then,

$$r = \frac{l}{2\tan\frac{\theta}{2}} \tag{4.4}$$

For a reflector with 6 ribs, each 21.4 mm wide, Equation 4.4 gives $r = 18.5$ mm. Similarly, for 12 ribs ($\theta = 30°$), $r = 40$ mm and for 24 ribs ($\theta = 15°$), $r = 82$ mm.

Two different analyses have been carried out. First, by extracting the natural frequencies immediately after applying the prestress, without first checking that equilibrium is satisfied. This is the most straightforward, although not fully correct method of analysis. Second, by carrying out a series of equilibrium iterations before extracting the frequencies. This allows the membrane and ribs to settle down, but achieving the intended state of prestress is by no means a trivial achievement.

4.2.1 Analysis without Equilibrium Check

An initial uniaxial prestress of 100 N/m is applied in the hoop direction, in each gore, but no initial moments are applied in the ribs. In the dummy static analysis step the nodes along the ribs are restrained. Then, in the frequency analysis step, the boundary conditions are released while the nodes at the base of the ribs are restrained using the **BOUNDARY, OP=NEW* option. In this analysis, the membrane prestress remains constant because no equilibrium iteration is carried out; therefore there the ribs remain unstressed.

The natural frequencies of a 10 m diameter reflector were analysed for different hub radii. Detailed results are presented in Sections 4.4.1 - 4.4.4, including a comparison of the natural frequencies of a 1.5 m diameter reflector with 6 ribs, computed using the equivalent truss model approach.

4.2.2 Analysis with equilibrium check

As the above analysis does not represent the actual stress state of the reflector, a more careful analysis of a 1.5 m diameter reflector with 6 ribs has been carried out, including an equilibrium iteration in the second step, i.e. before the linear frequency analysis step. The second step is a non-linear static analysis step, with the actual boundary conditions of the reflector.

When this second step is carried out, the membrane prestress applies uniform horizontal forces on the ribs, directed towards the axis of the reflector. Therefore, the ribs bend inwards, like the curved cantilever shown in Figure 4.4, but this causes a loss of prestress in the membrane. To maintain the original shape and prestress distribution, this deformation should be avoided. Therefore, it is necessary to apply the corresponding bending moments as initial bending moments in the ribs; their values can be calculated either analytically —from simple equilibrium consideration— or by using ABAQUS. There is an approximation involved in doing this as, even though the bending moment varies along a rib, only average values can be applied in each rib element. The results are shown in Section 4.4.5 and discussed in Section 4.5.5.

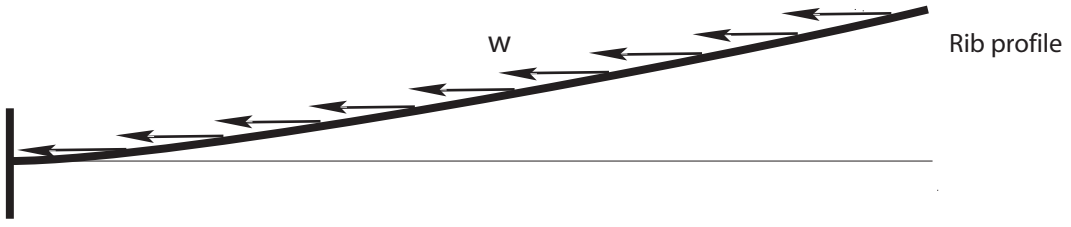

Figure 4.4: Profile of a rib with uniform loads.

4.3 Results

4.3.1 Reflector with Smallest Possible Hub

The first fifteen natural frequencies of a 1.5 m diameter reflector with three different numbers of ribs are tabulated in Table 4.2. The prestress is 100 N/m in the hoop direction. The first nine mode shapes of the reflector with 6 ribs are plotted in Figures 4.5 and 4.6.

Table 4.2: Natural frequencies of 1.5 m diameter reflectors with $F/D = 0.78$.

Mode	Frequency (Hz)		
	6 ribs	12 ribs	24 ribs
1	16.46	17.78	17.40
2	16.46	17.78	17.40
3	17.51	18.05	20.64
4	17.51	18.05	20.64
5	22.16	27.93	29.22
6	23.57	27.93	29.22
7	23.71	37.66	41.50
8	24.61	37.66	41.50
9	24.61	39.87	41.95
10	25.04	42.11	43.95
11	25.04	42.11	43.95
12	29.78	42.13	43.97
13	31.59	42.13	43.97
14	31.59	42.13	43.98
15	34.67	42.13	43.98

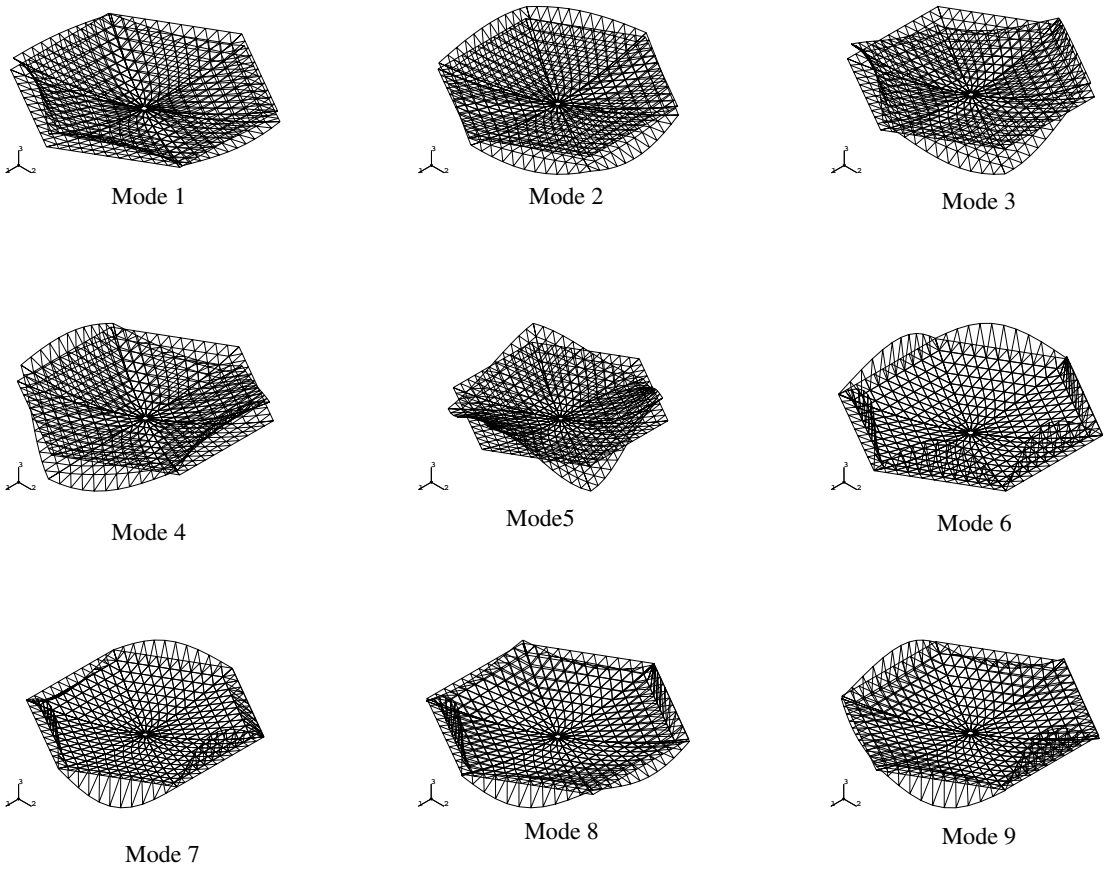

Figure 4.5: Mode shapes of 1.5 m diameter reflector with 6 ribs.

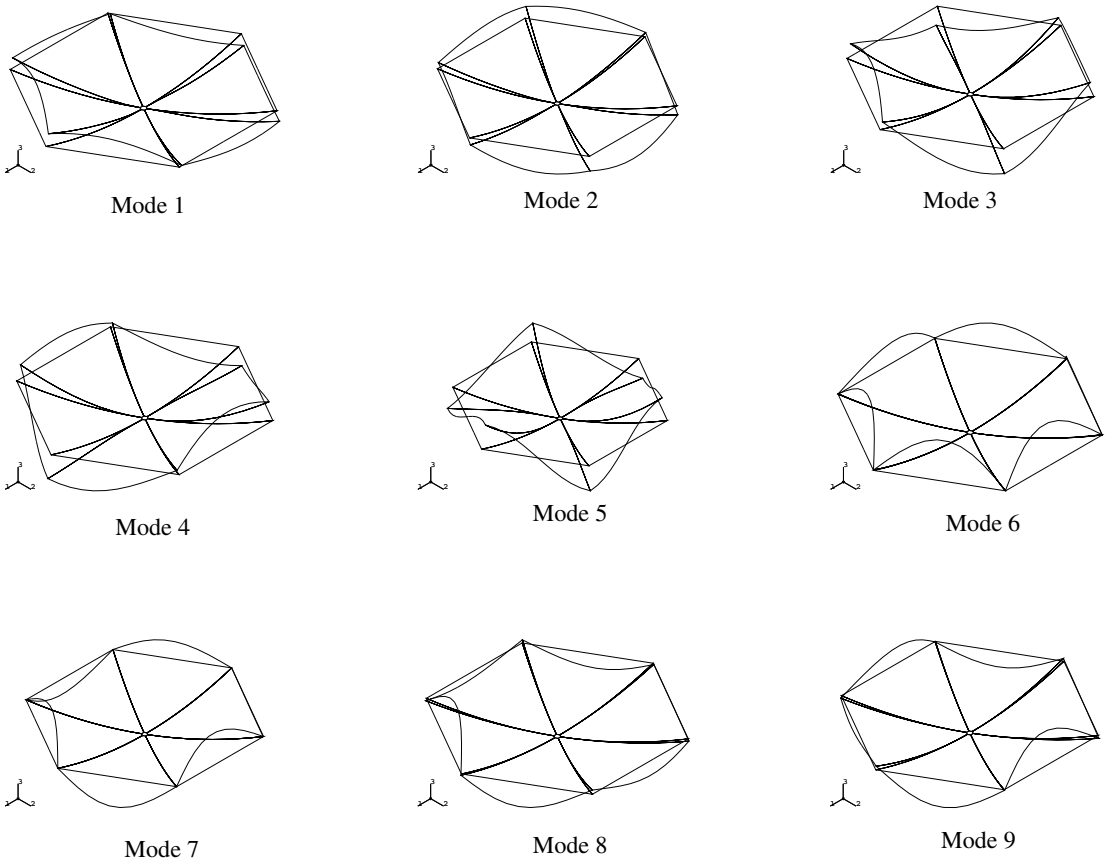

Figure 4.6: Outline of mode shapes shown in Figure 4.5.

Table 4.3 lists the first fifteen natural frequencies of a 5 m diameter reflector with three different numbers of ribs. The first nine mode shapes of the reflector with 12 ribs are plotted in Figures 4.7 and 4.8.

Table 4.3: Natural frequency of 5 m diameter reflector with $F/D = 0.78$.

Mode	Frequency (Hz)		
	6 ribs	12 ribs	24 ribs
1	3.14	2.97	2.85
2	3.14	2.97	2.85
3	5.09	4.55	4.01
4	5.09	4.55	4.01
5	6.74	6.60	5.96
6	6.89	6.60	5.96
7	7.12	8.61	8.04
8	7.47	8.61	8.04
9	7.47	9.41	10.18
10	7.54	10.36	10.18
11	7.54	10.39	11.87
12	7.60	10.39	12.33
13	8.49	11.30	12.33
14	9.00	13.75	12.69
15	9.30	14.18	14.43

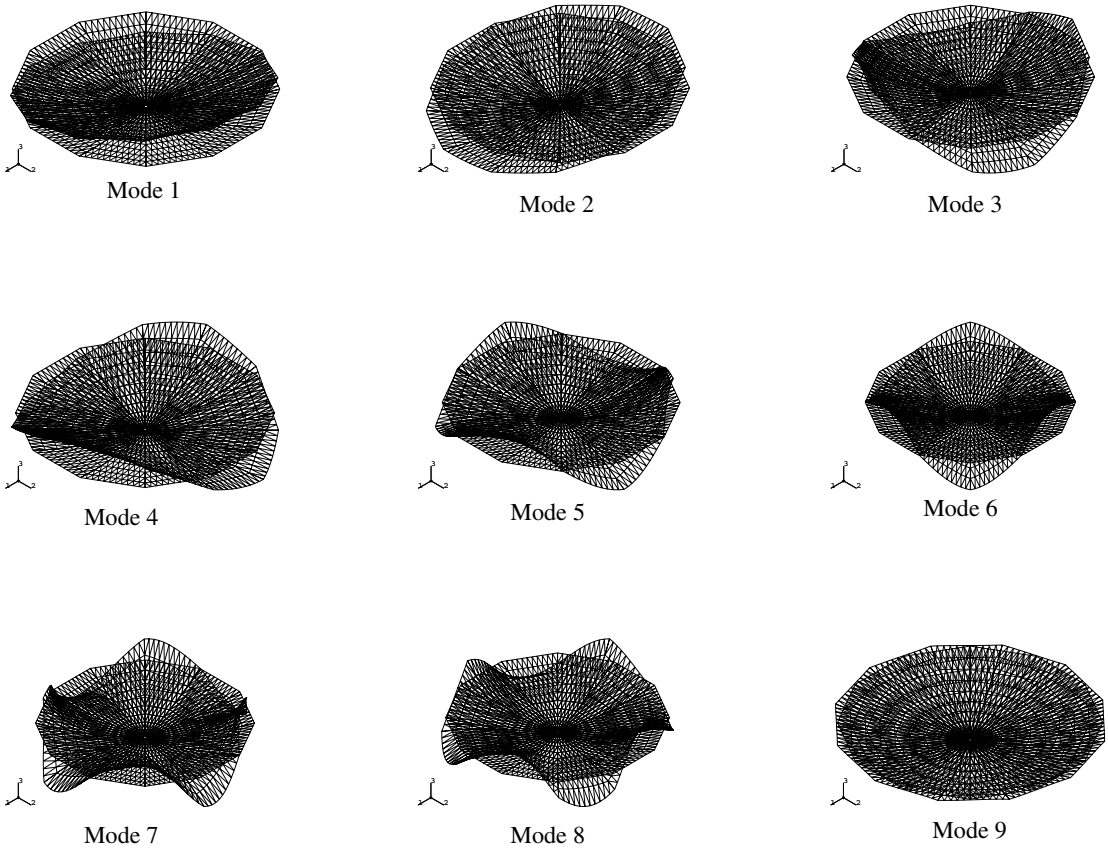

Figure 4.7: Mode shapes of 5 m diameter reflector with 12 ribs.

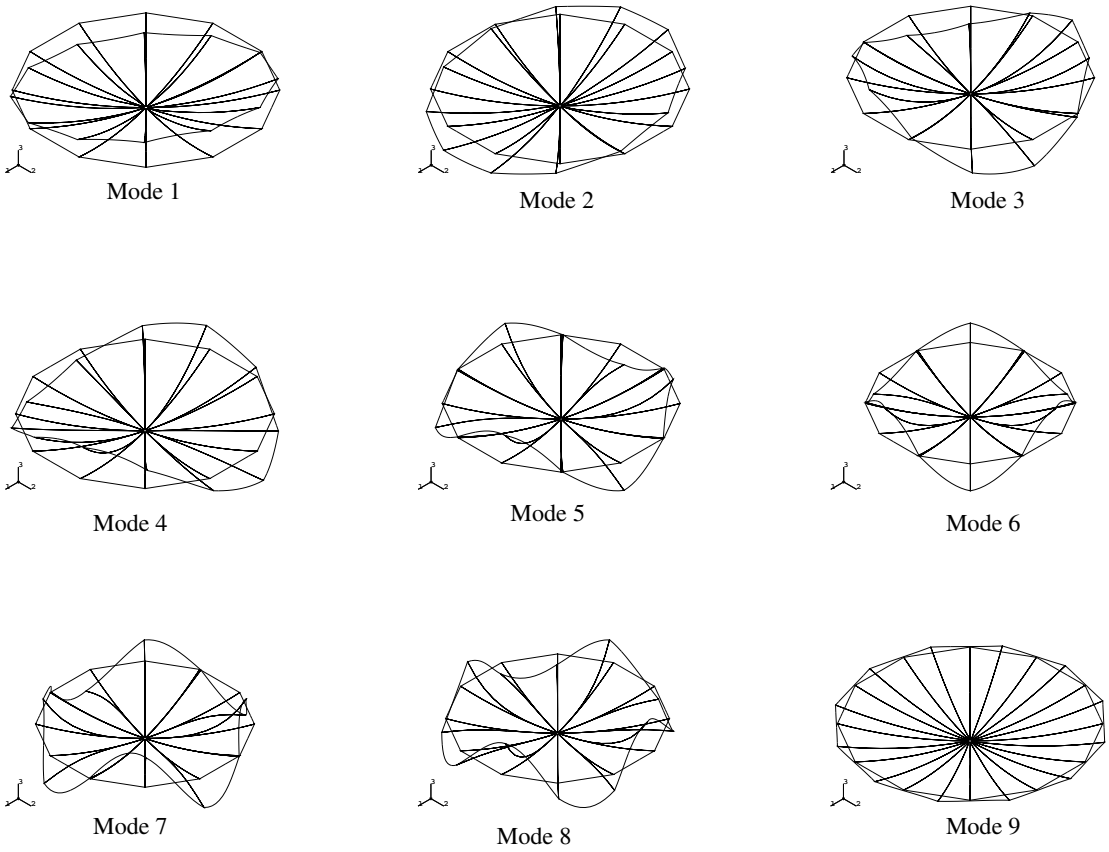

Figure 4.8: Outline of mode shapes shown in Figure 4.7.

Table 4.4 shows the first fifteen natural frequencies of a 10 m diameter reflector with different numbers of ribs. The first nine mode shapes for 24 ribs are plotted in Figures 4.9 and 4.10.

Table 4.4: Natural frequency of 10 m diameter reflector with $F/D = 0.78$.

Mode	Frequency (Hz)		
	6 ribs	12 ribs	24 ribs
1	1.54	1.43	1.32
2	1.54	1.43	1.32
3	2.72	2.47	2.23
4	2.72	2.47	2.23
5	2.78	3.35	3.21
6	2.93	3.48	3.21
7	3.56	3.56	3.99
8	3.74	3.56	4.21
9	3.75	4.63	4.21
10	3.75	4.63	4.57
11	3.76	5.63	5.21
12	3.84	5.63	5.21
13	3.84	6.26	6.21
14	4.52	6.87	6.21
15	4.56	6.98	7.20

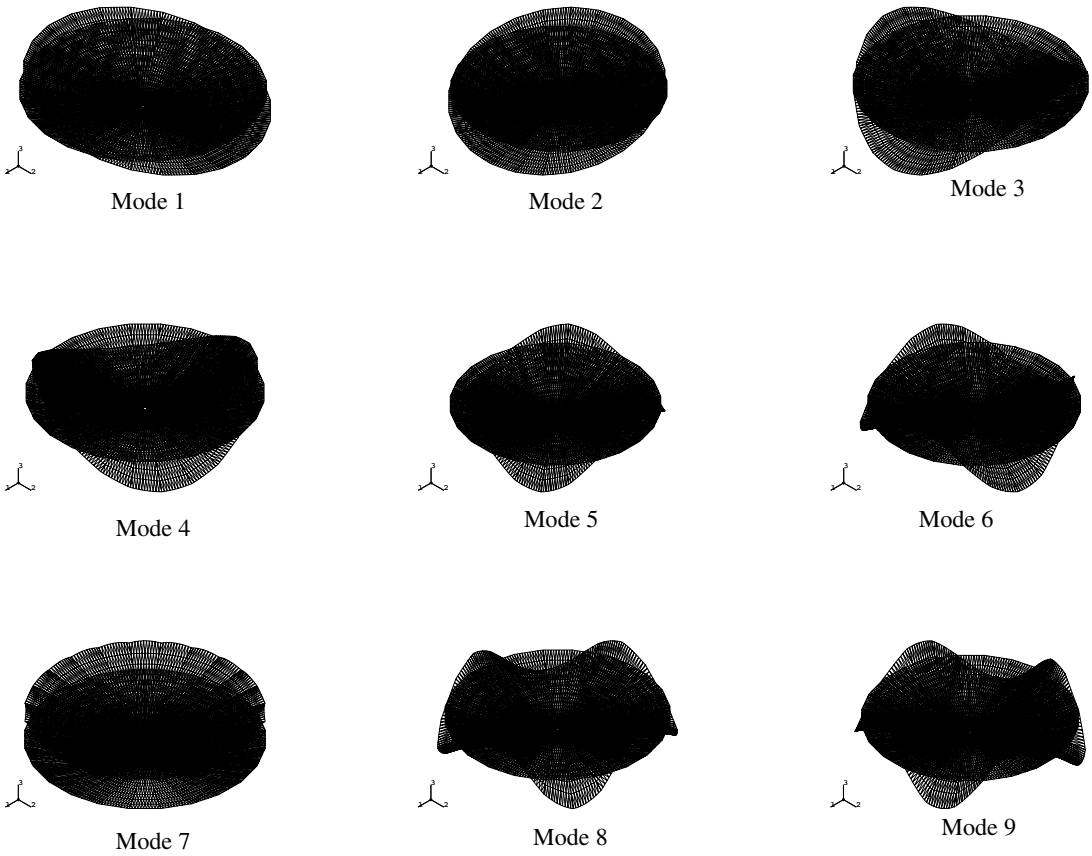

Figure 4.9: Mode shapes of 10 m diameter reflector with 24 ribs.

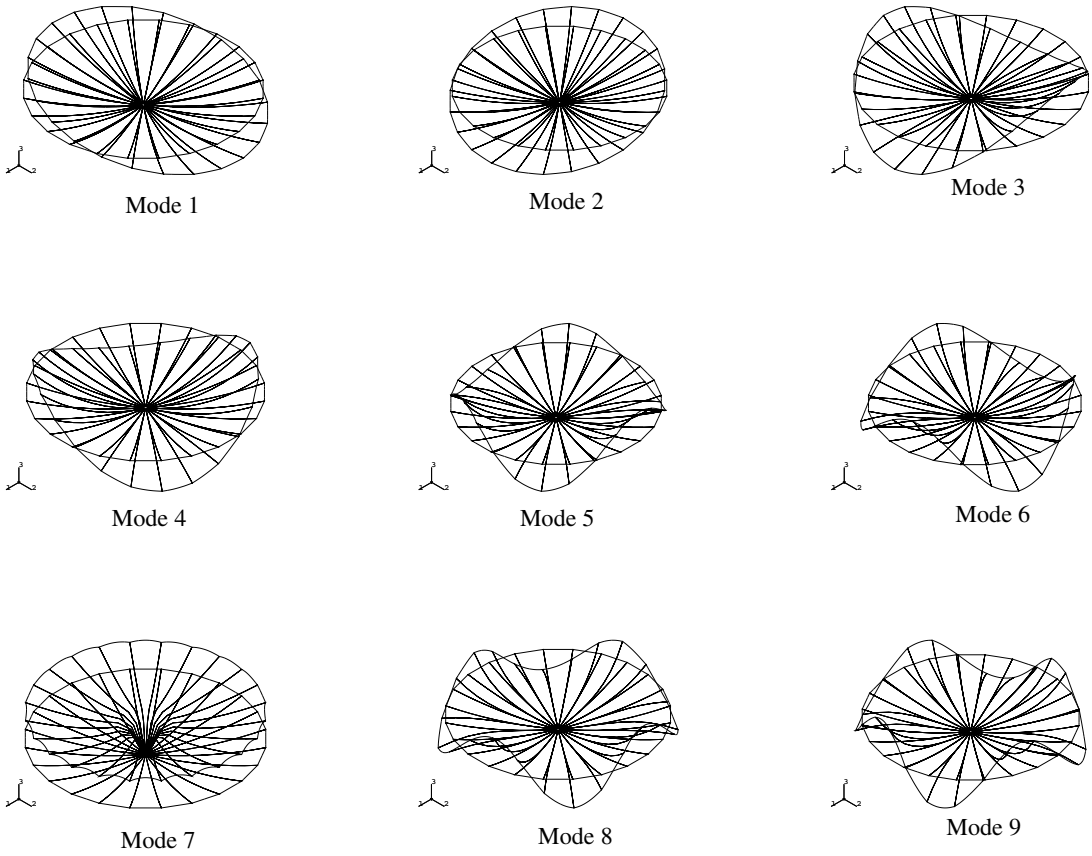

Figure 4.10: Outline of mode shapes shown in Figure 4.9.

4.3.2 10 m Reflector with Different Hub Sizes

The first nine natural frequencies of the 10 m diameter reflector have been calculated for different hub radii. Detailed results are given in Table 4.5.

Table 4.5: Natural frequencies of 10 m diameter reflector with different hub radii.

Mode	Frequency (Hz)								
	6 ribs			12 ribs			24 ribs		
	20mm	40mm	80mm	40mm	80mm	160mm	82mm	150mm	300mm
1	1.54	1.54	1.55	1.43	1.44	1.46	1.32	1.34	1.42
2	1.54	1.54	1.55	1.43	1.44	1.46	1.32	1.34	1.42
3	2.72	2.71	2.72	2.47	2.47	2.47	2.23	2.23	2.23
4	2.72	2.72	2.72	2.47	2.47	2.47	2.23	2.23	2.23
5	2.78	2.91	3.07	3.35	3.41	3.56	3.21	3.21	3.21
6	2.93	3.56	3.56	3.49	3.56	3.56	3.21	3.21	3.21
7	3.56	3.75	3.75	3.56	3.56	4.17	3.99	4.21	4.21
8	3.74	3.75	3.75	3.56	4.63	4.63	4.21	4.21	4.21
9	3.75	3.76	3.76	4.63	4.63	4.63	4.21	4.45	5.21

4.3.3 Variation of Frequency with Prestress

The natural frequencies of 1.5 m diameter reflectors with minimum hub radius and hoop prestress of 50, 100 and 200 N/m have been calculated. The results are tabulated in Table 4.6.

Table 4.6: Natural frequency of 1.5 m diameter reflector with different prestress.

Mode	Frequency (Hz)								
	Stress = 50N/m			Stress = 100N/m			Stress = 200N/m		
	6 ribs	12 ribs	24 ribs	6 ribs	12 ribs	24 ribs	6 ribs	12 ribs	24 ribs
1	14.63	15.87	16.14	16.46	17.78	17.40	18.27	19.12	19.56
2	14.63	15.87	16.14	16.46	17.78	17.40	18.27	19.12	19.56
3	14.65	17.37	20.30	17.51	18.05	20.64	21.66	20.96	21.21
4	14.65	17.37	20.30	17.51	18.05	20.64	21.66	20.96	21.21
5	16.72	24.94	27.48	22.16	27.93	29.22	27.02	32.28	32.12
6	16.77	24.94	27.48	23.57	27.93	29.22	33.08	32.28	32.12
7	17.98	30.91	39.15	23.71	37.66	41.50	33.54	39.64	42.11
8	17.98	30.91	39.15	24.61	37.66	41.50	34.49	41.84	44.09
9	18.87	32.04	41.87	24.61	39.87	41.95	34.49	41.84	44.09

4.3.4 Comparison of Membrane and Truss Models

The natural frequencies of a 1.5 m diameter reflector with 6 ribs have been calculated by two different approaches. First, naturally the membrane elements and second with a triangular framework of pin-jointed elements, as explained in Section 3.1.3. The results are tabulated in Table 4.7.

Table 4.7: Comparison of natural frequencies of 1.5 m diameter reflector with 6 ribs.

Mode	Frequency (Hz)	
	Membrane Model	Truss Model
1	16.46	16.11
2	16.46	16.11
3	17.51	17.06
4	17.51	17.06
5	22.16	21.75
6	23.57	22.87
7	23.71	22.92
8	24.61	22.95
9	24.61	22.95

The first nine mode shapes are plotted in Figure 4.11.

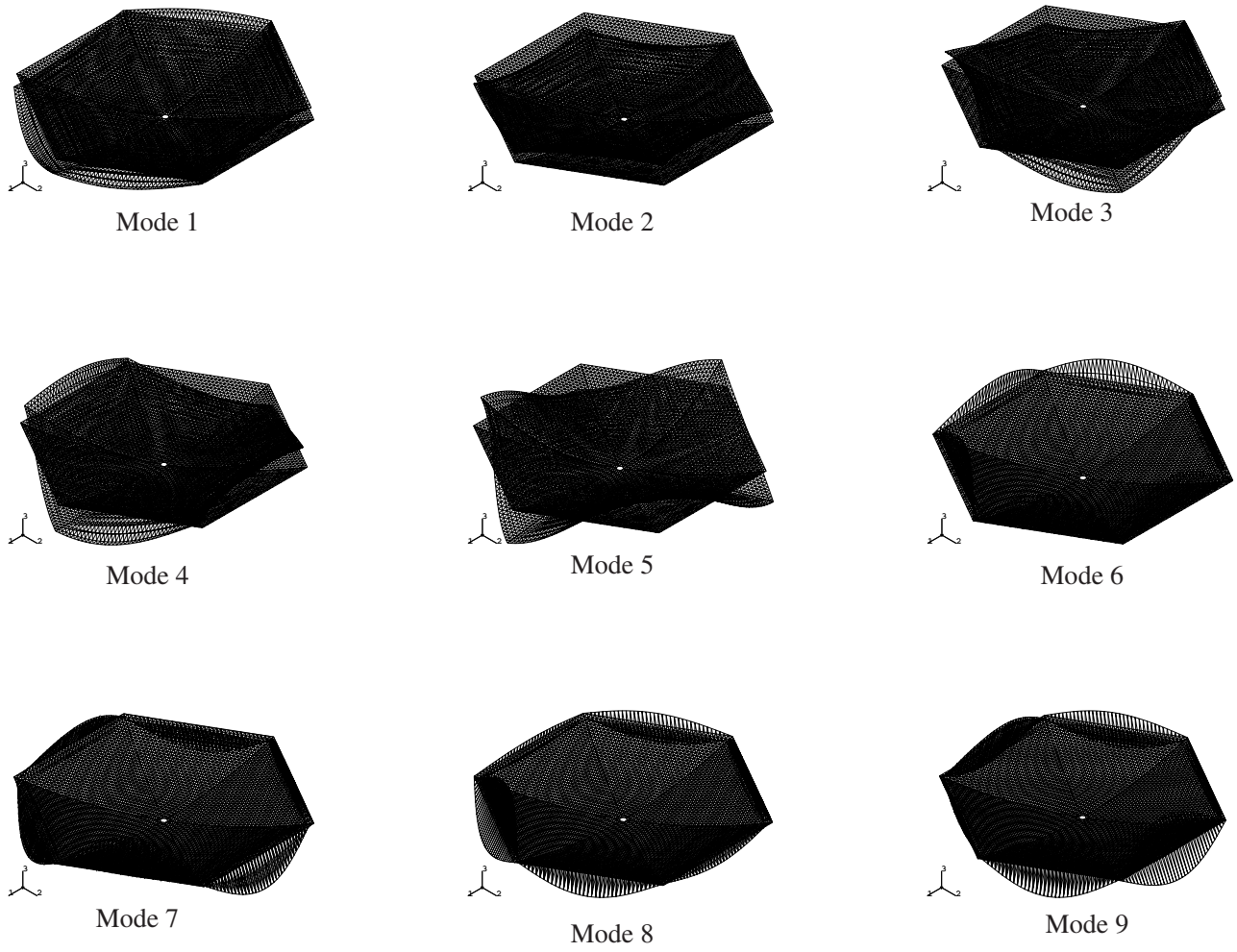

Figure 4.11: Mode shapes of 1.5 m diameter reflector with 6 ribs modelled as a framework.

4.3.5 1.5 m Reflector with Equilibrium Check

The natural frequencies of a 1.5 m diameter reflector with 6 ribs have been analysed. Membrane prestress levels between 100 N/m and 30 N/m have been applied, with the corresponding bending moments on the ribs, but the membrane prestress is 40 N/m or above, ABAQUS fails to converge during the equilibrium check (it is thought that this is due to buckling of the ribs). Therefore, the analysis has been completed only for a prestress of 30 N/m. The results are plotted in Figures 4.12 and 4.13.

The plot of hoop stress in Figure 4.12 shows that most of the membrane is under tension, except for a very small portion near the hub of the reflector. The stress values decrease continuously from the outer edge towards the hub. Almost half of the outer surface remains close to the applied prestress of $30 \times 10^5 N/m^2$,

corresponding to 30 N/m, but towards the hub the stress rapidly decreases and the smallest tensile stress is approximately ten times smaller than the applied initial stress. As the distance between two adjacent ribs decreases, near the hub, the reduction of prestress increases. Efforts to improve the stress distribution are continuing at the time of writing.

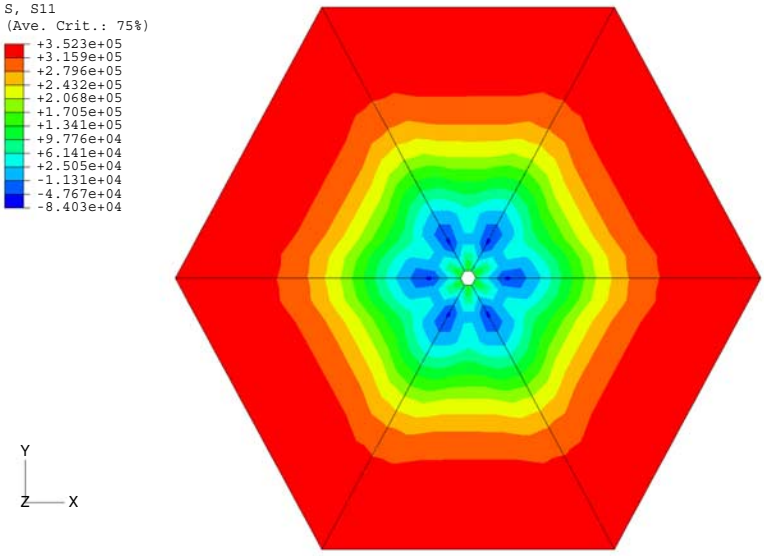

Figure 4.12: Hoop stress of 1.5 m diameter reflector with 6 ribs for prestress of 30 N/m.

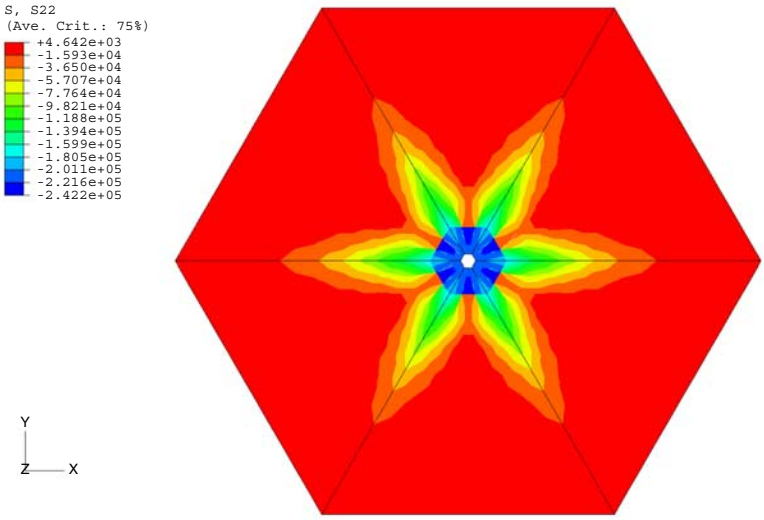

Figure 4.13: Radial stress of 1.5 m diameter reflector with 6 ribs for prestress of 30 N/m.

The radial stress plot in Figure 4.13 shows a considerable zone of compressive stress near the hub and along the ribs. This effect is related through Poisson's ratio to the loss of hoop prestress already discussed.

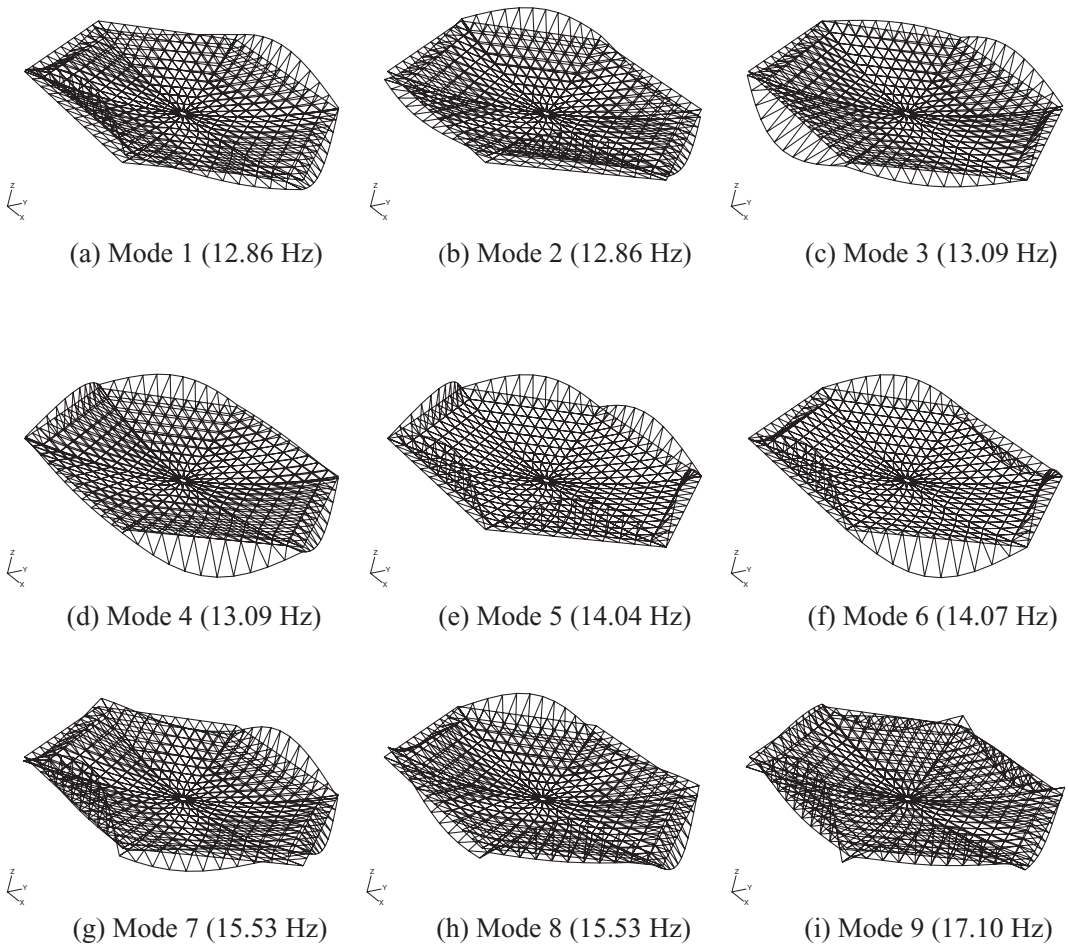

(a) Mode 1 (12.86 Hz) (b) Mode 2 (12.86 Hz) (c) Mode 3 (13.09 Hz)

(d) Mode 4 (13.09 Hz) (e) Mode 5 (14.04 Hz) (f) Mode 6 (14.07 Hz)

(g) Mode 7 (15.53 Hz) (h) Mode 8 (15.53 Hz) (i) Mode 9 (17.10 Hz)

Figure 4.14: Mode shapes of CRTS Reflector of 1.5 m diameter with 6 ribs.

The first nine mode shapes of the model are plotted in Figure 4.14. Consecutive modes have equal frequencies but different mode shapes. This is related to the periodic nature of the reflector.

4.4 Discussion

The natural frequency variation of the 1.5 m diameter reflector with the number of ribs is shown in Table 4.2. Generally frequencies increase with the number of ribs, although a slight reduction is seen in the first two frequencies of the reflectors with 12 and 24 ribs.

Table 4.3 shows that the natural frequency of a 5 m diameter reflector decreases when the number of ribs is increased, but a variation to this pattern is observed for the last three modes. The same behaviour is observed —Table 4.4— also for

the first four modes of the 10 m diameter reflector, but only a complex variation is observed for the remaining modes.

The natural frequency of a structure depends on its stiffness and mass. When the number of ribs is changed, both the stiffness and mass of the reflector change. This explains why the behaviour discussed above does not show a single trend. It should also be noticed that in increasing the number of ribs no attempt has been made to optimise the design of the structure, e.g. by decreasing the cross-section of the ribs or increasing the level of prestress.

It is also observed that the natural frequencies of the reflector decrease when the diameter is increased. This is because both the stiffness of the reflector decreases and the mass of the reflector increases.

An important common feature is that two different modes exist at a given natural frequency. It can also be seen that the number of ribs in a reflector is equal to the number of normal modes observed in a group, e.g. a 6 rib reflector has 6 normal modes in a group and a 12 rib reflector has 12 normal modes in a group, although the number of natural frequencies in a group is less than the number of ribs. This observation confirms that the number of normal modes in a given propagation zone is equal to the number of substructures or identical repetitive units. This observation agrees with the observation made by SenGupta [13], already discussed in Section 2.3.

Table 4.5 shows that the natural frequencies of the 10 m diameter reflector do not change greatly with the hub radius, although in a very few cases it is not. Overall, a small increase in frequency is observed when the hub radius is increased.

Table 4.6 shows that the natural frequencies of 1.5 m diameter reflectors with initial stress of 50, 100, 200 N/m increases with the increase of prestress. The increase of frequency is less in the lower modes than in the higher modes.

Table 4.7 shows the natural frequencies of 1.5 m diameter reflectors (6 ribs) with membrane and framework elements. Similar results are observed from both types of analysis, which is reassuring. This confirms the accuracy of the membrane model.

It was expected that hoop stress should be 30 N/m uniformly throughout the membrane, with practically no stress in the radial direction. But, after carrying out the equilibrium iteration the stress distribution is found to be considerably different.

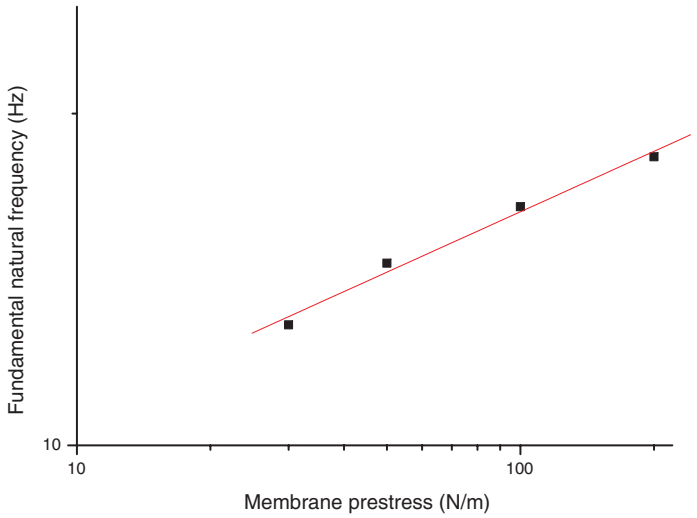

Figure 4.15: Variation of fundamental natural frequency with membrane prestress for 1.5 m diameter reflector with 6 ribs.

Figure 4.15 is a logarithmic plot of the fundamental natural frequency (without equilibrium iteration) of the 1.5 m diameter reflector with 6 ribs vs. the applied prestress. Because of the approximately linear fit, we have

$$y = 0.16x + 0.89 \tag{4.5}$$

which can be written as,

$$f \propto T^{0.16} \tag{4.6}$$

where f is fundamental natural frequency and T the membrane prestress.

If one considers the variation in frequency due to including the equilibrium iterations, this relationship becomes

$$f \propto T^{0.18} \tag{4.7}$$

It turns out that the fundamental natural frequency of the reflector with and without equilibrium iterations is not significantly different. Therefore it is reasonable to decide not to carry out this tedious additional analysis in a preliminary design situation.

Chapter 5

Conclusion

A numerical study of the vibration behaviour of CRTS reflectors has been done. The natural frequencies generally increase with the number of ribs and prestress level, but increase in frequency is less for lower modes than for higher modes decrease with the diameter of the reflector, and practically unaffected by the diameter of the hub.

An important common feature that has been observed is the existence of two different modes at a given natural frequency, and hence of an infinity of modes at the same frequency, obtained by taking a linear combination of the two modes given by ABAQUS. It has also been observed that the number of normal modes in a given propagation zone is equal to the number of ribs, but the number of natural frequencies is less than the number of normal modes. This clearly shows the periodic nature of the reflector.

5.1 Further Work

Because of the periodic nature of symmetric CRTS reflectors, they will be very sensitive to even small irregularities due to manufacturing and material tolerances.

Such irregularities can affect the vibration behaviour significantly, by localising the vibration modes and confining the energy to a region close to the source. Mode localisation in symmetric CRTS reflectors could cause the numerical predictions of their natural frequencies and mode shapes to be completely incorrect. Therefore an experimental analysis of the CRTS reflector will be required.

Bibliography

[1] Blevins, A. *Formulas for Natural Frequencies and Mode shapes.* Krieger Publishing Company, USA, 1995.

[2] Clough, R. W., and Penzien, J. *Dynamics of Structures.* McGraw-Hill, Inc, 1993.

[3] Cook, R. D., Malkus, D. S., and Plesha, M. E. *Concepts and Applications of Finite Element Analysis.* John Wily & Sons, New York, USA, 1989.

[4] Cornwell, P. J., and Bendiksen, O. O. Localization of vibrations in large space reflectors. *AIAA Journal 27*, 2 (1989), 219–226.

[5] Craig, R. R. *Structural Dynamics.* John Wiley and Sons, 1981.

[6] Graff, K. F. *Wave motion in elastic solids.* Clarendon Press, Oxford, 1975.

[7] Hibbit and Karlsson and Sorensen, Inc. *ABAQUS/Standard User's Manuals, Version 5.8.* USA, 1998.

[8] Hrennikoff, S. Solution of problems of elasticity by the framework method. *Journal of Applied Mechanics, Transactions of the ASME 8* (1941), 169–175.

[9] Nour-Omid, B. Applications of the Lanczos method. *Computer Physics Communications 53* (1989), 157–168.

[10] Phaal, R. *A two-surface computational model for the analysis of thin shell structures.* PhD thesis, University of Cambridge, 1990.

[11] Rayleigh, J. W. S. *Theory of Sound*, vol. 1. Dover Publications, Inc., New York, 1945.

[12] SenGupta, G. Natural flexural waves and the normal modes of periodically-supported beams and plates. *Journal of Sound and Vibration 13*, 1 (1970), 89–101.

[13] SenGupta, G. Vibration of periodic structures. *Shock and Vibration Digest 12*, 3 (1980), 17–31.

[14] Yap, D., and Cebon, D. Energy confinement in imperfect periodic systems. *Journal of Sound and Vibration 232*, 4 (2000), 669–694.

Appendix A

Sample ABAQUS Script

The following ABAQUS script was written to find out the fundamental natural frequency of the flat membrane shown in Figure 3.2 by using membrane elements.

```
*HEADING
MEMBRANE
Units: N m kg
*NODE
1, 0.0, 0.0, 0.0
11, 0.100, 0.0, 0.0
201, 0.0, 0.100, 0.0
211, 0.100, 0.100, 0.0
*NGEN, NSET=A1
1, 11, 1
*NGEN, NSET=A2
201, 211, 1
*NSET, NSET=A3, GENERATE
1, 201, 20
*NSET, NSET=A4, GENERATE
11, 211, 20
*NFILL
A1, A2, 10, 20
*ELEMENT, TYPE=M3D4
1, 1, 2, 22, 21
*ELGEN, ELSET=B1
1, 10, 1, 1, 10, 20, 10
*MEMBRANE SECTION, ELSET=B1, MATERIAL=KEVLAR
1E-4
*MATERIAL, NAME=KEVLAR
*DENSITY
790
```

```
*ELASTIC, TYPE=ISOTROPIC
11.9E9, 0.3
*INITIAL CONDITIONS, TYPE=STRESS
B1, 10E4, 10E4
*RESTART, WRITE
*STEP, NLGEOM
*STATIC
*BOUNDARY
A2, ENCASTRE
A4, ENCASTRE
A1, ENCASTRE
A3, ENCASTRE
*EL PRINT,POSITION=INTEGRATION POINT,FREQ=0
*EL FILE, FREQ=0,POSITION=INTEGRATION POINT
*NODE FILE, FREQ=0
*NODE PRINT, FREQ=0
*END STEP
*STEP
*FREQUENCY, EIGENSOLVER=LANCZOS
1
*BOUNDARY, OP=NEW
A1, 2
A3, 1
A4, 3
A2, 3
1, 1, 2
*EL PRINT, POSITION=INTEGRATION POINT, FREQUENCY=0
*EL FILE, FREQ=0,POSITION=INTEGRATION POINT
*NODE FILE, FREQ=0
*NODE PRINT, FREQ=0
*END STEP
```